Vol 11 No 11, November 2002
1009-1963/2002/11(11)/1175-04

Chinese Physics

© 2002 Chin. Phys. Soc.
and IOP Publishing Ltd

Dispersive properties of tunnelling-induced transparency in an asymmetric double quantum well*

Su Xue-Mei(苏雪梅)[a)b)c)], Zhuo Zhong-Chang(卓仲畅)[a)],
Wang Li-Jun(王立军)[b)c)], and Gao Jin-Yue(高锦岳)[a)†]

[a)] *Department of Physics, Jilin University, Chuangchun* 130023, *China*
[b)] *Changchun Institute of Optics, Fine Mechanics and Physics, Chinese Academy of Sciences, Changchun* 130021, *China*
[c)] *Laboratory of Excited State Process, Chinese Academy of Sciences, Changchun* 130021, *China*

(Received 9 April 2002)

We have investigated the dispersive properties of tunnelling-induced transparency in asymmetric double quantum well structures where two excited states are coupled by resonant tunnelling through a thin barrier in a three-level system of electronic subbands. The intersubband transitions exhibit high dispersion at zero absorption, which leads to the slow light velocity in this medium as compared with that in vacuum (c=3×10^8). The group velocity in a specific GaAs/AlGaAs sample is calculated to be $v_g=c/4.30$. This structure can be used to compensate for the dispersion and energy loss in fibre optical communications.

Keywords: Fano interference, double quantum well, dispersion
PACC: 4250, 7340L

The effect of Fano interferences on absorption and emission profiles has been used as the basis to achieve a laser without population inversion.[1] It is one of the numerous schemes for a laser without inversion (LWI).[2] It can expand the range of laser devices in mid-infrared to far-infrared spectral regions if we use the intersubband transitions in quantum wells.[3] Fano interference[4] occurs when a quasi-discrete excited state is coupled to a continuum. In such a system, the absorption spectrum exhibits a dip with zero absorption while the emission spectrum does not show a corresponding dip if the excited state is populated (pumped) incoherently. Since these frequencies are situated at the wing of the emission line, the effect is not very pronounced. Harris[5] has shown that an additional quasi-discrete state may produce a dramatic amplification of this effect. The scheme was demonstrated between autoionizing levels in Zn vapour by Hahn *et al.*[6] Although Harris[5] had in mind atomic systems, he also suggested that in tunnelling systems nonreciprocal line shapes should exist as well.

Fano interference in intersubband transitions in quantum wells can be used for the application of LWI[3,7] as well as optical switching.[8] Recently, several observations of tunnelling-induced transparency in intersubband absorption through Fano interference in a semiconductor double quantum well structure have been reported.[9−11] These were made by applying an ultra-thin potential-energy barrier through which two intermediate states that arise from the mixing of the states in two adjacent semiconductor quantum wells, are broadened by tunnelling into the same energy continuum (see Fig.1). In the latter papers, the dispersive properties of the transparency via Fano interference have not been involved. For similar three or more level systems where coherence is maintained by the external electromagnetic field[12−14] in an atomic system, Harris and co-workers have discussed the dispersive properties and predicted a reduction in the group velocity of a pulsed probe beam. A further experiment succeeded in a reduction of the pulse propagation velocity to 17m/s.[15]

In this paper, we calculate the dispersive properties of tunnelling-induced transparency and the reduction of group velocity in an asymmetric coupled semiconductor quantum well structure, as shown in Fig.1.

Figure 1 shows the schematic band diagram for the semiconductor structure. The states of the shal-

*Project supported by the National Natural Science Foundation of China (Grant Nos 10074021 and 6007815) and by the Doctoral Programme Foundation of Institution of Higher Education China (Grant No 19201038).
†Author to whom any correspondence should be addressed.

low and deep wells are coupled by a thin tunnel barrier to form a doublet that interacts with the energy continuum. Levels $|2\rangle$ and $|3\rangle$ are characterized by their decay rates to the continuum and their oscillator, or equivalently by their Rabi frequencies to level $|1\rangle$. The interference arises between the absorption paths through two resonances to the continuum. The absorption interference leads to a linear rapidly varying refractive index with a reduction in the group velocity. The slow group velocity is the result of the high dispersion and not of the magnitude of the refractive index.

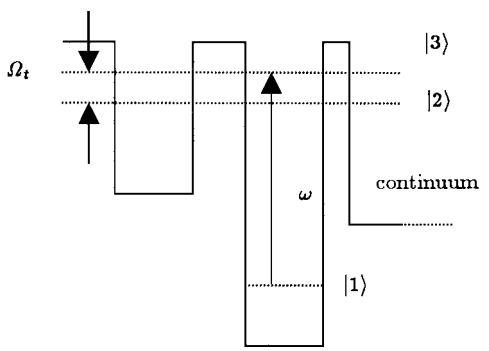


Fig.1. Schematic energy-level diagram of a GaAs/$Al_xGa_{1-x}As$ coupled quantum well structure used to demonstrate the quantum interference in optical absorption from the ground state $|1\rangle$ in a deep well to the doublet $|2\rangle$ and $|3\rangle$, which are coupled to a continuum by a thin tunnel barrier adjacent to the deep well. Also shown are the coherent coupling strength Ω_t and the probe field $\hbar\omega$.

The Hamiltonian operator for the system shown in Fig.1 is defined as $H = H_0 + H_i$, where H_0 is the field-free Hamiltonian and H_i is the interaction of the electron with the electromagnetic field. In the interaction picture, the individual contributions of Hamiltonians may be expressed as the following matrix elements:

$$\begin{aligned} H_i^{32} &= -\hbar\Omega_{32}\mathrm{e}^{\mathrm{j}\omega_{32}t}, \\ H_i^{31} &= -\frac{\hbar}{2}\Omega_{31}\mathrm{e}^{\mathrm{j}(\omega_{31}-\omega)t}, \\ H_i^{21} &= -\frac{\hbar}{2}\Omega_{21}\mathrm{e}^{\mathrm{j}(\omega_{21}-\omega)t}, \end{aligned} \tag{1}$$

Here, the rotating-wave approximation is used, and only resonant terms have been included. $\mu_{\mathrm{mn}} = \mathrm{e}\langle m|z|n\rangle$ are dipole-moment matrix elements for the transition $m \leftrightarrow n$ with a linear polarization, and $\Omega_{21} = \mu_{21}E/\hbar$ and $\Omega_{31} = \mu_{31}E/\hbar$ are the respective Rabi frequencies. The wavefunction of the system in the interaction picture is expressed as

$$|\Psi(t)\rangle = a_1(t)|1\rangle + a_2(t)|2\rangle + a_3(t)|3\rangle, \tag{2}$$

where a_1, a_2 and a_3 represent the amplitudes of $|1\rangle$ and the resonances $|2\rangle$ and $|3\rangle$ respectively. Inserting Hamiltonian (1) into the Schrödinger equation $|\dot{\Psi}(t)\rangle = -\frac{\mathrm{j}}{\hbar}H|\Psi(t)\rangle$, we obtain

$$\begin{aligned} &\dot{a}_1(t)|1\rangle + \dot{a}(t)|2\rangle + \dot{a}_3(t)|3\rangle \\ &= \mathrm{j}\Big(\frac{1}{2}\Omega_{21}a_1\mathrm{e}^{\mathrm{j}(\omega_{21}-\omega)t}|2\rangle + \frac{1}{2}\Omega_{21}a_2\mathrm{e}^{-\mathrm{j}(\omega_{31}-\omega)}|1\rangle \\ &\quad + \frac{1}{2}\Omega_{31}a_1\mathrm{e}^{\mathrm{j}(\omega_{31}-\omega)t}|3\rangle + \frac{1}{2}\Omega_{31}a_3\mathrm{e}^{-\mathrm{j}(\omega_{31}-\omega)t}|1\rangle \\ &\quad + \Omega_{32}a_3\mathrm{e}^{-\mathrm{j}\omega_{32}t}|2\rangle + \Omega_{32}a_2\mathrm{e}^{\mathrm{j}\omega_{32}t}|3\rangle\Big). \end{aligned} \tag{3}$$

From Eq.(3), we have the equations:

$$\begin{aligned} \dot{a}_1 &= \frac{\mathrm{j}}{2}\Omega_{21}a_2\mathrm{e}^{-\mathrm{j}(\omega_{21}-\omega)t} + \frac{\mathrm{j}}{2}\Omega_{31}a_3\mathrm{e}^{-\mathrm{j}(\omega_{31}-\omega)t}, \\ \dot{a}_2 &= \frac{\mathrm{j}}{2}\Omega_{21}a_1\mathrm{e}^{\mathrm{j}(\omega_{21}-\omega)t} + \mathrm{j}\Omega_{32}a_3\mathrm{e}^{-\mathrm{j}\omega_{32}t}, \\ \dot{a}_3 &= \frac{\mathrm{j}}{2}\Omega_{31}a_1\mathrm{e}^{\mathrm{j}(\omega_{31}-\omega)t} + \mathrm{j}\Omega_{32}a_2\mathrm{e}^{\mathrm{j}\omega_{32}t}. \end{aligned} \tag{4}$$

In order to solve Eq.(4), we define the slowly-varying amplitudes as:

$$\begin{aligned} b_1 &= a_1, \\ b_2 &= a_2\mathrm{e}^{-\mathrm{j}(\omega_{21}-\omega)t}, \\ b_3 &= a_3\mathrm{e}^{-\mathrm{j}(\omega_{31}-\omega)t}. \end{aligned} \tag{5}$$

It then follows from Eqs.(4) and (5) that

$$\begin{aligned} \dot{b}_1 &= \frac{\mathrm{j}}{2}\Omega_{21}b_2 + \frac{\mathrm{j}}{2}\Omega_{31}b_3, \\ \dot{b}_2 + \mathrm{j}\Delta\omega_{21}b_2 &= \frac{\mathrm{j}}{2}\Omega_{21}b_1 + \mathrm{j}\Omega_{32}b_3, \\ \dot{b}_3 + \mathrm{j}\Delta\omega_{31}b_3 &= \frac{\mathrm{j}}{2}\Omega_{31}b_1 + \mathrm{j}\Omega_{32}b_2, \end{aligned} \tag{6}$$

where $\Delta\omega_{21} = (\omega_{21} - \omega)$ and $\Delta\omega_{31} = (\omega_{31} - \omega)$ are defined as frequency detunings. ω is the photo frequency of the probe, and ω_{21} and ω_{31} are the transition frequencies between the ground state $|1\rangle$ and the two resonances. In Eqs.(6) the term $\mathrm{j}\Omega_{32}$ is used to describe the mutual coupling of states $|2\rangle$ and $|3\rangle$, which is the cross term $k_{23} = -\frac{1}{2}\sqrt{\Gamma_2\Gamma_3}$ as in Ref.[5], where Γ_2 and Γ_3 are the full widths at half maximum for $|2\rangle$ and $|3\rangle$ respectively, which are proportional to the tunnelling rates into the continuum. Considering the decaying processes, the frequency detunings $\Delta\omega_{21}$ and $\Delta\omega_{31}$ in Eqs.(6) must be replaced by the complex frequency detunings $\Delta\tilde{\omega}_{21} = \Delta\omega_{21} - \mathrm{j}\Gamma_2/2$ and $\Delta\tilde{\omega}_{31} = \Delta\omega_{31} - \mathrm{j}\Gamma_3/2$. Then the probability amplitude equations describing the system are obtained

$$\dot{b}_1 = \frac{\mathrm{j}}{2}\Omega_{21}b_2 + \frac{\mathrm{j}}{2}\Omega_{31}b_3,$$

$$\dot{b}_2 + \mathrm{j}\Delta\tilde{\omega}_{21} b_2 = \frac{\mathrm{j}}{2}\Omega_{21} b_1 + k_{23} b_3,$$
$$\dot{b}_3 + \mathrm{j}\Delta\tilde{\omega}_{31} b_3 = \frac{\mathrm{j}}{2}\Omega_{31} b_1 + k_{23} b_2. \qquad (7)$$

Steady-state solutions are obtained by setting the time derivatives given in Eqs.(7) equal to zero and the approximation $|b_1|^2 \approx 1$. The complex macroscopic susceptibility can be solved by the formula $P = N(\mu_{12} b_2^* b_1 + \mu_{13} b_3^* b_1)$. With the definition $P = \varepsilon_0 \chi(\omega) E(\omega)$, the expression of the linear susceptibility is

$$\chi(\omega) = \frac{N}{\varepsilon_0 \hbar} \frac{2(\mu_{13}^2 \Delta\omega_{21} + \mu_{12}^2 \Delta\omega_{31}) - \mathrm{j}(\mu_{12}^2 \Gamma_3 + \mu_{13}^2 \Gamma_2 + 4\mu_{12}\mu_{13} k_{23})}{4\Delta\omega_{21}\Delta\omega_{31} - 2\mathrm{j}(\Gamma_2 \omega_{31} + \Gamma_3 \Delta\omega_{21})}, \qquad (8)$$

where N is the density of electrons in the material.

The formula could be put in a compact form by using the normalized energy detunings $\eta_2 = -\Delta\omega_{21}/(\Gamma_2/2)$, $\eta_3 = -\Delta\omega_{31}/(\Gamma_3/2)$, and the parameter $q = \dfrac{\mu_{13}}{\mu_{12}}\sqrt{\dfrac{\Gamma_2}{\Gamma_3}}$ which controls the magnitude of the interference effect. Inserting the expressions η_2, η_3 and q into Eq.(8), we obtain the normalized imaginary and real parts of the susceptibility:

$$\mathrm{Im}\chi = \frac{(\eta_3 + \eta_2 q)^2}{\eta_2^2 \eta_3^2 + (\eta_2 + \eta_3)^2},$$
$$\mathrm{Re}\chi = \frac{\eta_2\eta_3(\eta_3 + \eta_2 q^2) + (q-1)^2(\eta_2 + \eta_3)}{\eta_2^2 \eta_3^2 + (\eta_2 + \eta_3)^2}. \qquad (9)$$

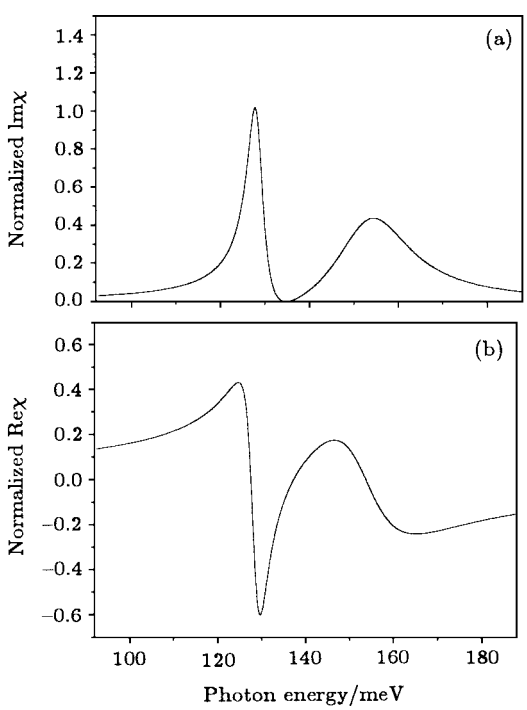


Fig.2. (a) Imaginary and (b) real parts of the susceptibility of a probe frequency ω in the semiconductor structure shown in Fig.1. The parameters are $\Gamma_2 = 5.0$meV, $\Gamma_3 = 20$meV, $\Omega_t = 26.5$meV, q=0.66. The curve is normalized to the peak value of the imaginary part of the susceptibility.

The absorption and dispersive profiles predicted by Eq.(9) are depicted in Fig.2, where the parameters used are from the sample of $GaAs/Al_{0.15}Ga_{0.85}As$, as in Ref.[8]. We notice that, at zero absorption, the refractive index of the probe light is close to unity and the large dispersion is positive, but it is negative at the absorption maximum. These properties lead to the following: (1) the propagation of the probe light in the sample is similar to that in vacuum without any loss; (2) the dispersion at zero absorption can be used to compensate the dispersion in the travelling medium, and therefore this technique possesses a potential application in optical communications; (3) the slowing down of the group velocity at zero absorption is expected, which is the result of the rapid change in the refractive index due to the absorption interference induced by the tunnelling effect. These results show that this semiconductor structure is useful to compensate dispersion and energy loss in fibre optical communications if appropriate parameters for quantum wells are chosen.

We take ω_0 equal to the frequency of the probe at zero absorption. The value of the real and imaginary parts of the susceptibility and the derivatives evaluated at this frequency can be calculated from Eq.(9). The group velocity for the propagating electromagnetic pulse is

$$v_g = \frac{c}{n(\omega_0) + \omega_0 \dfrac{\mathrm{d}n}{\mathrm{d}\omega}(\omega_0)}, \qquad (10)$$

where n and $\mathrm{d}n/\mathrm{d}\omega$ is the refractive index and the dispersion at ω_0 the frequency respectively. We calculate the group velocity of the sample as in Ref.[8] using Eq.(10), and the result is $v_g = c/4.30$.

From Eqs.(9) and (10), we notice that the parameter q not only controls the magnitude of the interference[11] but also the magnitude of the dispersion at ω_0; therefore it controls the magnitude of the reduction of the group velocity. The effect of the parameter q on the light group velocity is demonstrated

in Fig.3. The curve in Fig.3 shows that the group velocity ratio, c/v_g, is linearly proportional to parameter q. Because the quantum well structures are artificially made, the reduction of the group velocity can be adjusted by the height and width of the tunnelling barrier, and thus the magnitude of interference.

In summary, we have demonstrated that the intersubband absorption interference induced by tunnelling in a coupled quantum well structure displays an anomalous dispersion with zero absorption, which could be used to compensate the phase shift in media. At the same time, this dispersion varies rapidly, and therefore leads to a reduction of group velocity of the probe light at zero absorption. Moreover, with the rapid development in the field of artificial quantum confinement structures, the precisely specified wavelengths used for the compensation can be chosen. By adjusting the height and width of the tunnelling barrier via a bias voltage, the magnitude of the reduction in group velocity can be controlled.

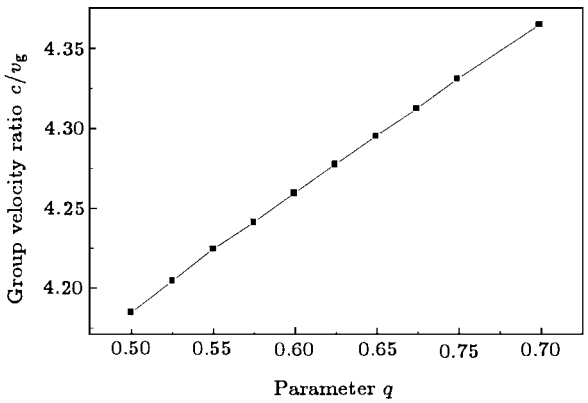


Fig.3. The group velocity ratio, c/v_g, via the parameter of the magnitude of the interference q.

References

[1] Akripin V G and Heller Y I 1983 *Phys. Lett.* **98A** 12

[2] Imamoglu A, Field J E and Harris S E 1991 *Phys. Rev. Lett.* **66** 1154
Agarwal G S 1991 *Phys. Rev.* A **44** R28
Gao J Y, Cuo C *et al* 1992 *Opt. Commun.* **93** 323
Gao J Y, Zhang H Z *et al* 1994 *Opt. Commun.* **110** 590
Padmabandu G G *et al* 1996 *Phys. Rev. Lett.* **76** 2053
Hu X M *et al* 1998 *Chin. Phys.* **7** 886

[3] Khurgin J B and Rosencher E 1996 *IEEE J. Quantum Electron.* **32** 1882

[4] Fano U 1961 *Phys. Rev.* **124** 1866

[5] Harris S E 1989 *Phys. Rev. Lett.* **62** 1033

[6] Hahn K H, King D A and Harris S E 1990 *Phys. Rev. Lett.* **65** 2777

[7] Imamoglu A and Ram R J 1994 *Opt. Lett.* **19** 1744

[8] Su X M and Gao J Y 2000 *Phys. Lett.* A **264** 346

[9] Faist J, Capasso F, Sirtori C, Hutchinson A L, West K W and Pfeiffer L N 1997 *Appl. Phys. Lett.* **71** 3477

[10] Schmidt H, Campman K L, Gossard A C and Imamoglu A 1997 *Appl. Phys. Lett.* **70** 3455

[11] Faist J, Capasso F, Sirtori C, West K W and Pfeiffer L N 1997 *Nature* (London) **390** 589

[12] Harris S E, Field J E and Kasapi A 1992 *Phys. Rev.* A **46** R29

[13] Xiao M, Li Y Q, Jin S Z and Julio Gea-Banacloche 1995 *Phys. Rev. Lett.* **74** 666

[14] Harris S E, Kasapi A, Maneesh Jain and Yin G Y 1995 *Phys. Rev. Lett.* **74** 2447

[15] Hau L V, Harris S E, Dutton Z and Behroozi C H 1999 *Nature* **397** 594